Available online at www.sciencedirect.com
ScienceDirect
Journal of Catalysis 243 (2006) 420–427
JOURNAL OF CATALYSIS
www.elsevier.com/locate/jcat

The role of PdZn alloy formation and particle size on the selectivity for steam reforming of methanol

Ayman Karim, Travis Conant, Abhaya Datye *

Department of Chemical and Nuclear Engineering and Center for Micro-Engineered Materials, University of New Mexico, Albuquerque, NM 87131, USA

Received 30 March 2006; revised 26 June 2006; accepted 21 July 2006

Abstract

Pd/ZnO has been shown in recent years to have high selectivity toward CO_2 during methanol steam reforming. It is commonly assumed that PdZn alloy formation is essential to achieve high selectivity toward CO_2. The simplest method for forming a PdZn alloy is to treat a Pd/ZnO catalyst at elevated temperatures in H_2, generally >350 °C. The high-temperature treatment, while transforming Pd to PdZn, also leads to particle growth. This makes it difficult to independently assess the role of particle size and composition on selectivity. In this work, we have used alternative activation treatments to vary independently the particle size and extent of alloy formation. XRD and TEM were used to obtain estimates of average crystallite size and composition. We found that even without any pretreatment, PdZn alloy particles were formed after reaction at 250 °C, due to the facile reduction of ZnO in the presence of Pd and H_2. Samples treated at low temperatures in H_2 showed the coexistence of monometallic Pd and PdZn alloy particles. Higher-temperature reduction led to complete transformation of Pd into the PdZn alloy. However, the selectivity toward CO_2 did not increase monotonically with the extent of alloy formation. Samples with low alloy content also showed CO_2 selectivity comparable to those with complete alloy formation. In each case, lower CO_2 selectivity was exhibited by samples containing small particles (∼1.5 nm). We conclude that one consequence of high-temperature reduction is elimination of these small particles, leading to improved selectivity. It was also surprising that an increase in PdZn alloy crystallite size with increasing reduction temperature had no adverse impact on catalyst reactivity.

Keywords: Methanol steam reforming; Pd/ZnO; PdZn alloy; TEM; XRD; Rietveld refinement

1. Introduction

Compact fuel cell systems operating with hydrocarbon fuels have high volumetric and gravimetric energy density and could outperform batteries in low-power portable electronics [1]. The challenge is to develop efficient microreformers for converting the chemical fuel into H_2, which can be fed to a proton-exchange membrane fuel cell to produce electricity. Among the fuels considered, methanol is an attractive candidate because it is sulfur-free and, most importantly, can be reformed at low temperatures (200–250 °C) [2]. The low reforming temperature results in low CO concentration (1.5%) in the product gases. This makes it possible, with elevated-temperature (180 °C) PEM fuel cells, to feed the reformate directly to the fuel cell without subsequent CO cleanup. Fuel cell membranes composed of polybenzimidazole (PBI) polymer allow high-temperature operation (up to 200 °C), and performance is not affected by CO concentrations up to 3% [3]. Most early studies focused on Cu-based catalysts, which exhibit high selectivity to CO_2 and H_2 [4]. However, Cu-based catalysts have the disadvantages of fast deactivation, poor thermal stability above 270 °C, and pyrophoric characteristics.

In contrast to Cu, methanol decomposition to CO and hydrogen is favored over group VIII metals, such as Pd [4]. On the other hand, Iwasa et al. [5] were the first to report that when supported on ZnO and reduced at temperatures higher than 300 °C, Pd showed high activity and selectivity to CO_2 and H_2. Iwasa et al. [6,7] postulated that during the reduction, H_2 spills over from Pd metal to reduce the ZnO and form PdZn alloy. The higher the reduction temperature, the greater the extent

* Corresponding author.
E-mail address: datye@unm.edu (A. Datye).

0021-9517/$ – see front matter
doi:10.1016/j.jcat.2006.07.024

of alloy formation and hence the higher the catalyst selectivity. Chin et al. [8] also showed that Pd/ZnO was less selective when reduced at 125 °C than when reduced at 350 °C; the difference in selectivity was again attributed to the presence of monometallic Pd particles when the catalyst was reduced at 125 °C compared with PdZn alloy particles after reduction at 350 °C. Reduction at 350 °C, while yielding higher selectivity, also led to an increase in particle size. Because methanol steam reforming is carried out at low temperatures, there is a need to synthesize catalysts with the highest reactivity. Pd/ZnO catalysts have a lower activity than copper-based catalysts. It is with this goal in mind that we set out to explore different activation treatments that might yield PdZn alloy particles with high dispersion.

In this work, we prepared a coprecipitated Pd/ZnO catalyst and subjected it to reductive treatment at temperatures up to 400 °C. The crystallite size and composition were studied using STEM, HRTEM, and whole-pattern Rietveld refinement of XRD data. As we show, some of the catalyst pretreatments allowed us to prepare catalysts in which both Pd and PdZn alloy particles were present, whereas higher-temperature reduction led to nearly complete alloy formation. We found that the catalysts with low selectivity always had particles 1–2 nm in size. Higher-temperature treatment led to particle growth, with improved in selectivity to CO_2. The phase content did not correlate directly with CO_2 selectivity. We conclude that the catalytic behavior of monometallic Pd supported on ZnO must be very different from that of Pd supported on SiO_2 or Al_2O_3, in which Pd shows very poor selectivity to CO_2 formation from methanol.

2. Experimental

2.1. Catalyst preparation

Because ZnO readily dissolves under acidic conditions, our Pd/ZnO catalyst was prepared by coprecipitation. First, ZnO powder (Aldrich) was dissolved in a 5 wt% Pd in nitric acid. The pH was then slowly adjusted to 9.5 using NaOH. The precipitate was filtered, washed, and dried at room temperature under vacuum overnight. The dried catalyst before calcination is designated "as-prepared" (AP). The nominal Pd loading was 15 wt%. Two additional catalysts were also prepared on an alumina support to clarify some of the observations in this work. The Pd/Al_2O_3 and $PdZn/Al_2O_3$ catalysts were prepared by an incipient wetness technique. The Al_2O_3 was prepared by calcining boehmite (Sasol) at 850 °C for 5 h. For the Pd/Al_2O_3, a solution of 10 wt% $Pd(NO_3)_2$ in nitric acid was added dropwise to the Al_2O_3, and the mixture was shaken to ensure even distribution; then the powder was dried at 80 °C. The process was repeated until 7.4 wt% Pd was achieved. For the $PdZn/Al_2O_3$, a solution of Pd and Zn nitrates (Pd/Zn molar ratio = 0.38) was added drop by drop to the Al_2O_3 and the powder was shaken to ensure even distribution, then the powder was dried at 80 °C. The process was repeated until 7.2 wt% Pd was achieved, corresponding to 11.6 wt% PdZn when complete alloy formation was achieved.

2.2. Reactivity measurements

Measurements of the steam reforming of methanol were performed in tubular packed-bed reactors. The reactor consisted of a 1.75-mm-i.d. quartz tube positioned in an insulated programmable oven. The temperatures of the reactor outer surface and the reactor inlet and outlet were measured. The reactor effluent stream passed through a gas-sampling valve, then through a condenser to trap unreacted water and methanol before reaching a digital mass flow meter, which allowed monitoring of total product dry gas flow. The effluent of the reactor was analyzed using a Varian CP-3800 gas chromatograph equipped with a Porapak Q column and a thermal conductivity detector, using helium as the carrier gas. The analysis of the gas-phase species CO_2, CO, and CH_3OH, along with a carbon balance, allowed calculation of the methanol conversion and CO_2 selectivity. The gas chromatograph was programmed to sample reactor product gases at 20-min intervals around the clock. The entire system was automated by Labview software and appropriate data acquisition hardware.

Material balance was done as follows. Using the methanol conversion and CO_2 selectivity and the reaction network stoichiometry, the total theoretical dry gas flow rate was calculated and compared with the reading of the mass flow meter. The error was $<10\%$ in all experiments. Before the reaction, the catalyst was pretreated under different conditions, as explained in Section 3. After pretreatment, the catalyst was brought to the reaction temperature of 250 °C under helium flow. A mixture of 1.1:1 molar water/methanol was then pumped using a syringe pump (Cole Parmer 74900) at 0.2 ml/h to an in-house built vaporizer operating at 130 °C. The vaporizer was optimized to ensure a stable flow rate and minimize fluctuations in the water–methanol molar ratio [9]. Samples were not injected into the gas chromatograph until 15–30 min after the water–methanol flow was started, to allow the flow rate to stabilize. Product distribution was monitored while the flow rate of the liquid water–methanol mixture was changed from low to high.

2.3. Catalyst characterization

Scanning and high-resolution transmission electron microscopy (STEM and HRTEM) were performed on a JEOL 2010F FASTEM field emission gun scanning transmission electron microscope. Powdered samples were analyzed by X-ray diffraction (XRD) using a Scintag Pad V diffractometer with DataScan 4 software (from MDI, Inc.) for system automation and data collection. Cu$K\alpha$ radiation (40 kV, 35 mA) was used with a Bicron Scintillation detector (with a pyrolitic graphite curved crystal monochromator). Data were analyzed with Jade 6.5 Software (from MDI, Inc.) using the ICDD (International Center for Diffraction Data) PDF2 database (rev. 2004) for phase identification. All catalyst characterization was performed after the catalyst had been used for reactivity measurements in steam reforming of methanol for 4 h except when stated otherwise. Full-pattern Rietveld refinement using Riqas 3.1 (MDI Inc.) was performed to quantify the amounts of Pd and PdZn phases and their particle sizes in these catalysts.

3. Results

3.1. Catalyst pretreatment

Aliquots of the as-prepared Pd/ZnO catalyst were exposed to hydrogen reduction at temperatures up to 400 °C before reactivity measurement in methanol steam reforming for 4 h. The first two treatments involved the catalyst in its as-prepared state; the rest involved calcination in air at 350 °C. The pretreatments were as follows:

(1) Ramped to 250 °C in He (30 sccm) at 15 °C/min, then treated in H_2 (30 sccm) for 2 h at 250 °C.
(2) Ramped to 250 °C in H_2 (30 sccm) at 5 °C/min, then held for 2 h.
(3) Calcined ex situ in air at 350 °C for 5 h.
(4) Calcined ex situ in air at 350 °C for 5 h, then ramped to 1 °C in He (30 sccm) at 15 °C/min, then treated in H_2 (30 sccm) for 2 h at 150 °C.
(5) Calcined ex situ in air at 350 °C for 5 h, then ramped to 250 °C in He (30 sccm) at 15 °C/min, then treated in H_2 (30 sccm) for 2 h at 250 °C.
(6) Calcined ex situ in air at 350 °C for 5 h, then ramped to 400 °C in He (30 sccm) at 15 °C/min, then treated in H_2 (30 sccm) for 2 h at 400 °C.

After each pretreatment, the catalyst was brought to the reaction temperature of 250 °C under He flow. Then the water–methanol mixture was introduced to measure the catalyst reactivity. In the following sections, these catalysts are labeled by their pretreatment; however, unless stated otherwise, all of the characterizations were done after the catalyst was exposed to the reaction conditions for 4 h.

3.2. X-ray powder diffraction

Fig. 1 shows the XRD patterns of the catalysts after methanol steam reforming at 250 °C for 4 h. For the as-prepared catalyst reduced (at 250 °C) following a helium ramp, both Pd metal and PdZn alloy peaks were clearly identified in the pattern at 2θ of 40.16° and 41.23°, respectively (ICDD card #46-1043 for Pd and #06-0620 for PdZn). On the other hand, the as-prepared catalyst reduced (at 250 °C) with a hydrogen ramp showed only PdZn(111) reflection at $2\theta = 41.23°$. The calcined catalyst showed a broad peak covering the Pd(111) and PdZn(111) peaks. The calcined catalysts reduced at different temperatures showed smaller a Pd peak and a narrower PdZn peak with increasing reduction temperature.

3.3. Rietveld refinement

Previous work on Pd/ZnO catalyst used XRD mainly for qualitative-phase identification of Pd and PdZn present in the catalysts [5,6,8]. In the present study, whole-pattern Rietveld refinement was performed on the XRD patterns to quantify the amounts of the different phases. To verify the accuracy of our Rietveld refinement algorithm, we prepared a test sample of the same catalyst used in this work. The test sample was prepared by calcining the as-prepared catalyst (15 wt% Pd/ZnO nominal loading) at 350 °C; no reactivity measurement was performed on this catalyst. The calcined catalyst should comprise only two phases: PdO and ZnO. The nominal PdO weight loading after calcination should be 16.9%. Fig. 2 shows the XRD pattern and the Rietveld refinement; the weighted residual error was 5%. The weight loading of PdO calculated from the refinement was 16.2% (±0.6%), in close agreement with the nominal loading.

Fig. 3 shows the Rietveld refinement of the XRD pattern for the catalyst reduced (at 250 °C) following a He ramp. The refinement confirms the existence of a significant amount of Pd metal (25%) in this sample. The weighted residual error for this refined pattern was 6.5%. The XRD patterns for the other catalysts were also refined, and similar errors were obtained. A summary of the phase and particle size data is given in Table 1. The Pd loading (wt%) was calculated taking into account the Pd present in both Pd and PdZn phases and the Zn in PdZn

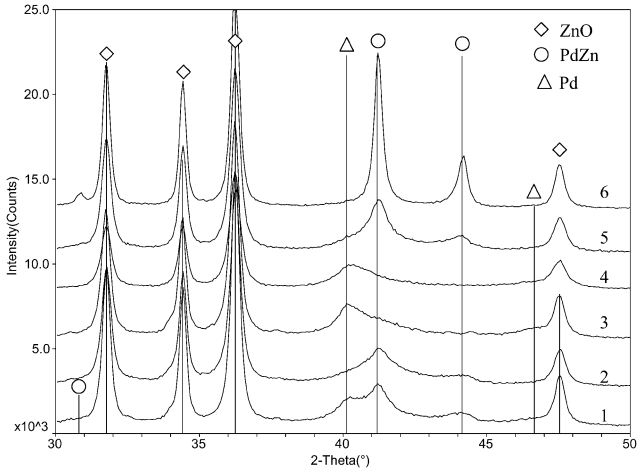

Fig. 1. XRD patterns of the Pd/ZnO catalysts with different pretreatments. (All XRD patterns were collected after reactivity measurements for 4 h.) Patterns labeled according to their pretreatment in Section 3.1.

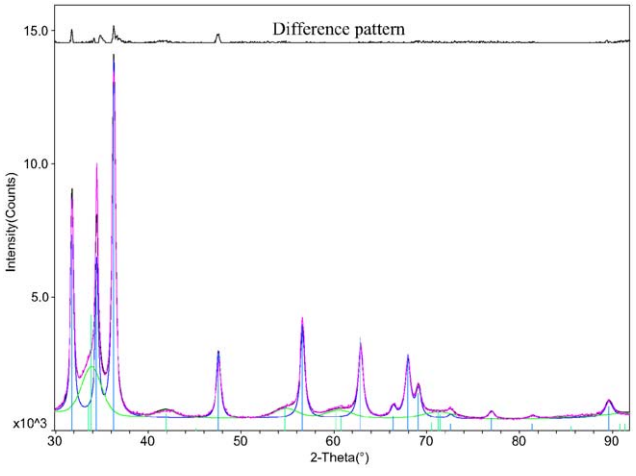

Fig. 2. XRD pattern and the Rietveld refinement for the test sample (PdO/ZnO). PdO in green, ZnO in blue, raw pattern in pink and the refined and difference patterns in black.

Table 1
Summary of the Rietveld refinement analysis

	Pretreatment					
	As-prepared		Calcined at 350 °C			
	1	2	3	4	5	6
H_2 reduction	250 °C (He ramp)	250 °C (H_2 ramp)	No prereduction	150 °C	250 °C	400 °C
Pd particle size (nm)	8.9	7.3	9.1	6.5	9.0	–
PdZn particle size (nm)	8.3	5.3	4.5	4.1	9.2	34.0
Pd/(Pd + PdZn) (wt/wt)	25%	16%	68%	75%	11%	0%
Pd/ZnO (wt/wt)	14.6%	14.2%	14.5%	15.5%	15.3%	14.0%

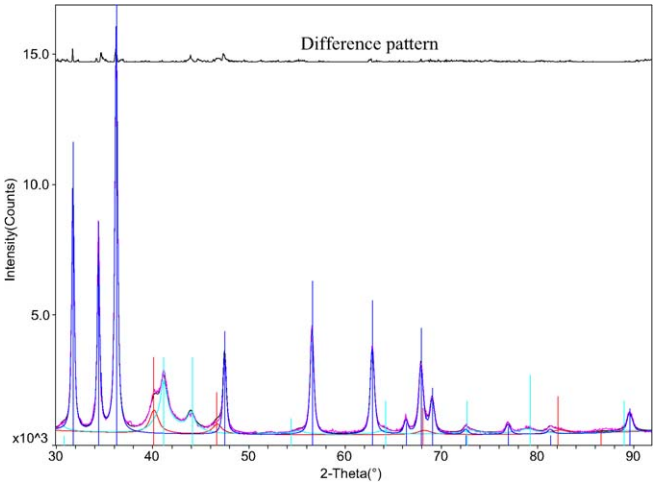

Fig. 3. Rietveld refinement of the catalyst reduced (at 250 °C) following a He ramp, pretreatment #1. (XRD pattern collected after reactivity measurements for 4 h.) ZnO in dark blue, PdZn in light blue, Pd in red, raw pattern in pink and the refined and difference patterns in black. (For interpretation of the references to colour in this figure legend, the reader is referred to the web version of this article.)

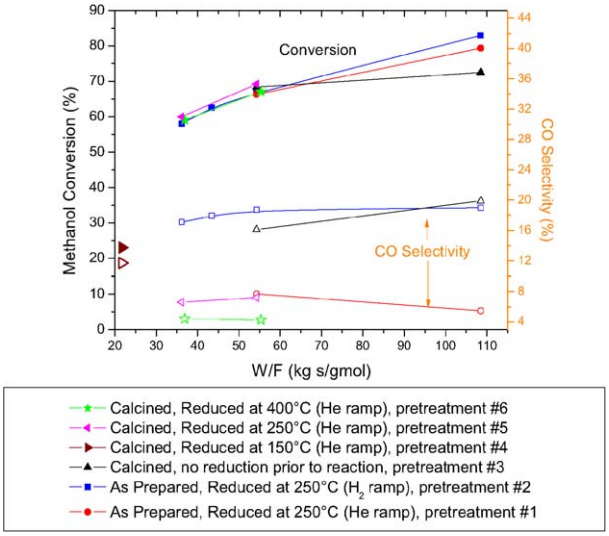

Fig. 4. Methanol conversion (filled symbols) and selectivity (open symbols). W/F = weight of catalyst/methanol molar flowrate. $P = 640$ Torr, $T = 250$ °C, H_2O/CH_3OH molar ratio = 1.1, CO selectivity = moles CO/(moles CO + CO_2) × 100.

and ZnO phases. The calculated Pd loading from XRD was very similar in all the catalysts and agrees very well with the nominal loading (15 wt%).

3.4. Methanol steam reforming

Fig. 4 shows the methanol steam-reforming reactivity results for the catalysts with different pretreatments. Selectivity and conversion are reported as a function of space-time (W/F) representing the weight of catalyst divided by the molar flow rate of reactants. CO selectivity is defined as mol of CO in the effluent divided by mol of CO + CO_2. The catalysts were stable for the duration of the test, with the selectivity to CO_2 increasing slightly with time on stream. The reactivity behavior can be related to the mean size and composition of these catalysts (as determined by XRD), because all sample characterization was done after the sample was used for reactivity measurements. As expected, the catalyst reduced at 400 °C showed the highest selectivity (96%) toward CO_2. However, another catalyst that showed separate Pd and PdZn peaks (from XRD) also exhibited a very high CO_2 selectivity (95%), close to the maximum selectivity (96%) achieved using this catalyst. Table 1 clearly shows that the relative amounts of Pd and PdZn in the catalyst do not necessarily determine the catalyst selectivity toward CO_2. This may appear to contradict what has been reported in the literature on Pd/ZnO catalysts, that complete PdZn alloy formation is necessary for high CO_2 selectivity [5,6,8]. The key difference, as we show in Section 3.5, is that the highly selective catalyst does not contain the smaller particles (1–2 nm diameter) that appear to lead to low selectivity. To ensure that these findings were reproducible, additional aliquots of the as-prepared sample were subjected to the pretreatments described here, and similar results were obtained. We also compared the behavior of the ZnO-supported catalysts with samples prepared on alumina. Fig. 10 shows the methanol conversion and CO selectivity of a 7.4% Pd/Al_2O_3 reduced at 400 °C and an 11.6% $PdZn/Al_2O_3$ reduced at 400 °C. The two catalysts exhibited particle sizes of 3–6 nm (using STEM). These data clearly show that the reaction rate for methanol decomposition on Pd was much lower than that for methanol reforming on PdZn under the same conditions. Monometallic Pd showed no selectivity to CO_2, whereas the $PdZn/Al_2O_3$ catalyst showed very high selectivity (98%).

3.5. Transmission electron microscopy

Because phase composition (determined by XRD) does not appear to determine selectivity, particle size distribution should

Table 2
Summary of phase and particle size analysis

	Pretreatment					
	As-prepared		Calcined at 350 °C			
	1	2	3	4	5	6
H_2 reduction	250 °C (He ramp)	250 °C (H_2 ramp)	No prereduction	150 °C	250 °C	400 °C
Pd particle size (nm) (XRD)	8.9	7.3	9.1	6.5	9.0	–
PdZn particle size (nm) (XRD)	8.3	5.3	4.5	4.1	9.2	34.0
Number average, diameter (nm) (STEM)	2.7	1.5	1.7	2.2	2.6	7.6
Volume average, diameter (nm) (STEM)	4.0	2.4	4.5	3.2	4.2	27.0
Pd/(Pd + PdZn) (wt/wt)	25%	16%	68%	75%	11%	0%
CO_2 selectivity	95%	83%	84%	88%	93%	96%

be carefully evaluated. Small particles provide most of the surface area and catalytic activity; hence TEM analysis is crucial for interpreting reactivity data. We used the high-angle annular dark field imaging (HAADF) technique in the STEM mode to enable detection of the smallest particles. We should point out that the presence of ZnO as a support makes it impossible to accurately quantify the Zn content of individual particles, particularly the smallest ones. We used elemental analysis via X-ray energy-dispersive spectroscopy for the larger particles and those that stick out from the support. We also determined the phase (Pd or PdZn) based on lattice fringe spacings in HRTEM images. Because the Pd and PdZn lattice spacings are very close, ZnO lattice spacings were used to provide an internal calibration.

Table 2 reports the particle sizes derived from STEM analysis along with the XRD average particle size, phase composition, and reaction selectivity. Clearly, for these catalysts, the average particle size obtained from STEM analysis is generally smaller than that obtained from XRD. This discrepancy is due to the inherent difference in how each technique averages the particle size. The XRD particle size represents a volume average of thousands of particles, but XRD tends to lose information from very small particles (<2 nm) due to peak broadening. In contrast, STEM images show the smallest particles that can be resolved in the microscope. Our STEM probe size is around 0.2 nm, but the low contrast of Pd and PdZn with respect to the support ZnO makes the smallest detectable particles about 1 nm in diameter. From the STEM images, we count a few hundred particles to determine an average size. A broad particle size distribution makes it difficult to accurately determine the relative numbers of small and large particles. One 20-nm-diameter particle has a Pd mass equal to that of 1000 2-nm-diameter particles. With only a few hundred particles analyzed, the larger particles will be undercounted in STEM analysis. Furthermore, larger particles are sometimes difficult to distinguish from the support, especially because the ZnO particle size is comparable to the larger Pd particles. Hence, when dealing with a broad particle size distribution, the particle size derived from XRD will be biased toward the larger particles, whereas the particle size from STEM will be biased toward the smaller particles.

We next examine the characteristics that distinguish those catalysts with low selectivity to CO_2. One of the catalysts exhibiting low selectivity to CO_2 was after treatment 2, which involved reduction at 250 °C following a H_2 ramp. Fig. 5a shows a representative STEM image of the catalyst, and Fig. 5b shows the particle size distribution (550 particles from 5 images). The number average and the volume average particle sizes were 1.5 and 2.4 nm, respectively. The average Pd loading using the standardless thin-film analysis via energy-dispersive spectroscopy was 12.9%. The metal loading results are in reasonable agreement with the Rietveld refinement, but the mean particle sizes are significantly different, due to the reasons explained above. The presence of significant numbers of small particles was found to be a key attribute of the catalysts exhibiting low selectivity to CO_2.

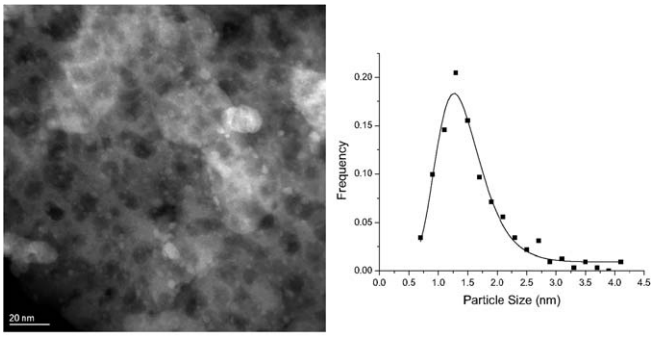

(a) STEM image (b) Particle size distribution

Fig. 5. Catalyst reduced (at 250 °C) with H_2 ramp, pretreatment #2. (Images taken after reactivity measurements for 4 h.)

Another catalyst showing low CO_2 selectivity was the calcined catalyst (treatment 3) containing about 68% monometallic Pd by weight (XRD particle size of 9.1 nm) and 32% PdZn by weight (XRD particle size of 4.5 nm). Fig. 6a shows a representative STEM image of this calcined catalyst, and Fig. 6b shows the particle size distribution. Although particles as large as 7 nm are shown in this STEM image, the size distribution derived from STEM fits a lognormal distribution with a single peak. The number average particle size is 1.7 nm. Fig. 7 shows a representative HRTEM image for the calcined catalyst. Because many of the lattice spacings for Pd and PdZn differ by <3%, we used ZnO as an internal standard to calibrate each image and to improve our ability to distinguish Pd from PdZn. For example, in Fig. 7, the ZnO(100) spacing (2.818 Å) was taken as an internal standard to calibrate the image. Pd(111) and PdZn(111) lattice spacings are 2.246 and 2.19 Å, respectively; therefore, the two particles with 2.25 Å lattice spacing were identified as Pd. This process was repeated for all of the images; each of the

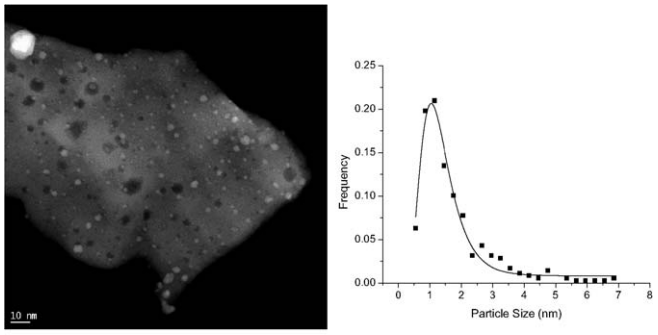

(a) STEM image (b) Particle size distribution

Fig. 6. STEM and particle size distribution of the calcined catalyst, pretreatment #3. (Images taken after reactivity measurements for 4 h.)

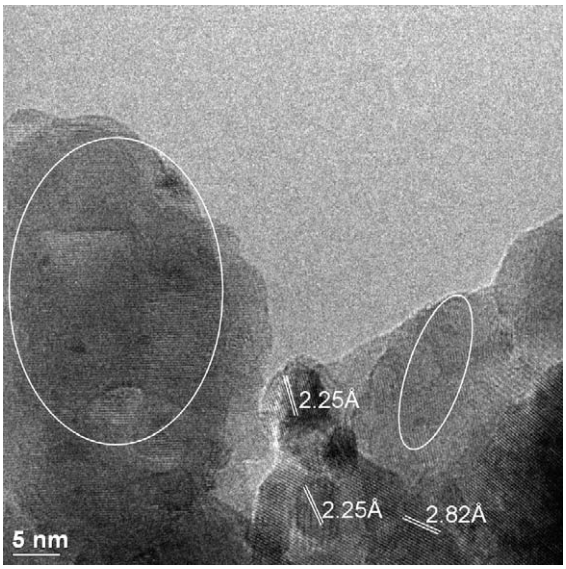

Fig. 7. HRTEM of the calcined catalyst, pretreatment #3. (Image taken after reactivity measurements for 4 h.)

particles identified in this manner had lattice fringes that could be indexed as monometallic Pd. Although lattice fringe images of these 3–4 nm particles can be readily obtained, it is very difficult (due to the contrast of the support) to measure lattice spacings of the smallest particles (0.7–1.5 nm) present in the areas highlighted in Fig. 7. This means that we cannot conclusively identify the phase of the smallest particles in this sample.

Results of STEM analysis of the catalysts showing higher CO_2 selectivity are presented in Figs. 8 and 9. In these figures, the peak of the size distribution and the number average size are larger than those shown in Figs. 5 and 6. Analysis of all of the samples in this set led us to conclude that catalysts showing high selectivity for reforming do not contain significant numbers of small particles (<2 nm diameter).

4. Discussion

The objective of the present work was to determine the role of particle size and phase composition on the reactivity for methanol steam reforming. We prepared one large batch of catalyst and varied the catalyst pretreatment to obtain catalysts with

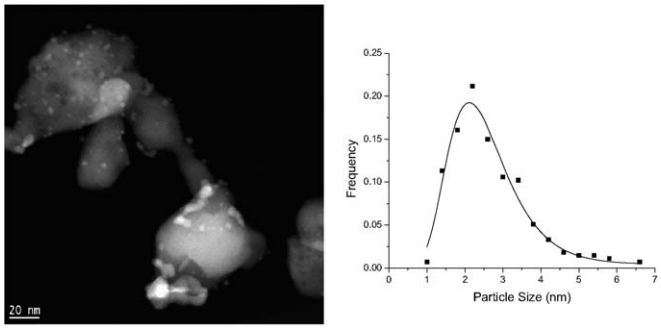

(a) STEM image (b) Particle size distribution

Fig. 8. STEM and particle size distribution of the catalyst reduced at 250 °C (He ramp), pretreatment #1. (Images taken after reactivity measurements for 4 h.)

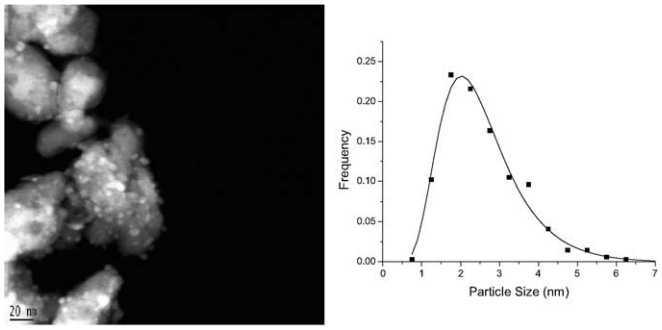

(a) STEM image (b) Particle size distribution

Fig. 9. STEM and particle size distribution of the calcined catalyst reduced at 250 °C (He ramp), pretreatment #5. (Images taken after reactivity measurements for 4 h.)

differing relative amounts of Pd and PdZn. The phase composition was determined by whole-pattern Rietveld refinement of XRD data. Varying the H_2 reduction temperature also allowed us to change the mean particle size. All of these catalysts had the same total metal content (Pd wt%).

Table 2 summarizes the Rietveld refinement, STEM analysis, and reactivity measurements. We can see that the selectivity toward CO_2 increased with the extent of alloy formation, but there are exceptions. Catalyst treatment 1 yielded 75% alloy formation and exhibited 95% selectivity toward CO_2. In contrast, catalyst treatment 2 with higher alloy content (84%) exhibited a lower selectivity toward CO_2 (84%). Likewise, catalyst treatments 1 and 6 yielded very similar selectivity and methanol conversion even with significantly different alloy contents (75 and 100%, respectively). This result is surprising, because monometallic Pd on alumina yields no CO_2, but favors methanol decomposition to CO and hydrogen (Fig. 10). How can we explain the high selectivity to CO_2 in catalysts containing significant amounts of monometallic Pd? One possible explanation is that Pd supported on ZnO behaves differently than Pd/Al_2O_3, favoring CO_2 formation rather than CO formation. Iwasa et al. [10] studied the selectivity of Pd/SiO_2, Pd/ZrO_2, and Pd/ZnO as a function of reduction temperature. Pd/SiO_2 showed 0% selectivity to CO_2 regardless of reduction temperature. The selectivity of Pd/ZnO increased with increasing reduction temperature, attributed to the PdZn alloy formation. However, Pd/ZrO_2 showed 35% selectivity toward CO_2

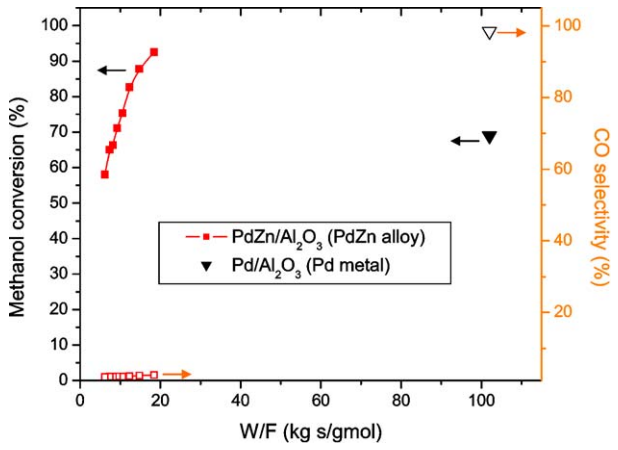

Fig. 10. Reactivity of Pd and PdZn supported on Al_2O_3. Methanol conversion (filled symbols) and selectivity (open symbols). W/F = weight of catalyst/methanol molar flowrate. $P = 640$ Torr, $T = 250\,^{\circ}C$, H_2O/CH_3OH molar ratio = 1.1.

with no PdZr alloy formation. Therefore, even without alloy formation, it was possible to modify the reaction selectivity of Pd particles by changing the support. A similar conclusion can be drawn from the work of Chin et al. [8], where the Pd/ZnO catalyst showed 90% selectivity toward CO_2 when reduced at 125 °C, far below the temperature required to form the PdZn alloy. Therefore, although their catalyst consisted mainly of monometallic Pd particles, the selectivity was as high as 90%. Our data confirm these findings; the calcined catalyst when reduced at 150 °C had about 75% Pd and still showed 88% selectivity toward CO_2. All of these results suggest that monometallic Pd particles supported on ZnO behave differently than Pd supported on SiO_2 or Al_2O_3, favoring CO_2 formation rather than CO formation. Our hypothesis is that monometallic Pd particles on ZnO exhibit high selectivity toward CO_2 because steam reforming of methanol proceeds on the interfacial sites between Pd and ZnO.

Another complementary factor leading to improved CO_2 selectivity of monometallic Pd catalysts is the low relative rate of the CO formation reaction. Fig. 10 shows that the rate for the methanol reaction was considerably slower on Pd/Al_2O_3 than on $PdZn/Al_2O_3$. But the low rate of CO production could be compensated for by a large surface area of the monometallic Pd. This appears to be the case with the catalysts that have a substantial fraction of particles in the 1–2 nm range. We can explain the low CO_2 selectivity of those catalysts as resulting from the large surface area of the Pd phase. As particle size grows, the relative importance of the Pd phase diminishes relative to the PdZn phase, especially because the intrinsic reactivity of Pd seems much lower than that of PdZn.

The electron microscopy and XRD data show that high-temperature reduction in H_2 led to significant particle growth. The high-temperature reduction also led to formation of the PdZn alloy. Electron microscope examination confirms that the larger particles all had an elemental analysis consistent with the PdZn structure. The XRD data also show a sharper peak for the PdZn phase as the catalyst was treated at elevated temperature. Consequently, we conclude that the role of high-temperature reduction is to enhance alloy formation and also to eliminate the small Pd particles; both actions help improve the selectivity of these catalysts. It also appears that the growth in particle size inevitably accompanies the transformation of Pd into the PdZn alloy. One factor is the increase in mass of an individual particle as Zn is alloyed with the Pd. It is surprising that the catalyst reactivity per gram for methanol steam reforming is unaffected by the growth in particle size occurring with high-temperature reduction. The catalyst treated at 400 °C (treatment 6) has a mean diameter of 34 nm but still provides the same conversion as the catalyst with a mean diameter of 9 nm (treatment 5). The loss of PdZn metal surface area seems to have no effect on overall reactivity. This means that either the reaction is structure sensitive, with large particles having higher intrinsic reactivity, or that the support ZnO contributes to the overall reactivity. Structure sensitivity is typically seen when particle sizes are varied over the range 1–10 nm; thus, we do not feel that the structure sensitivity of this reaction can explain the observed rate invariance with treatment temperature. Our hypothesis is that steam reforming of methanol is aided by the ZnO support. Future experiments using colloidal PdZn particles in the absence of the ZnO support may help clarify the role of the support in this reaction.

5. Conclusions

A coprecipitated Pd/ZnO catalyst was treated under conditions that led to the formation of separate Pd and PdZn nanoparticles coexisting on the support, with the extent of alloy formation ranging from 25% PdZn to 100% PdZn. By choosing the pretreatment conditions, it was possible to prepare catalysts containing significant fraction of particles <2 nm in diameter. We measured the rate for the methanol steam reaction and the product selectivity to CO or CO_2. It has been suggested in the literature that to achieve high CO_2 selectivity, high-temperature (350 °C) reduction is needed to transform all of the Pd to the PdZn alloy [5,8]. In contrast, our work shows that high CO_2 selectivity can also be achieved with lower reduction temperature, but only after the smallest particles (<2 nm) have been eliminated. We conclude that these small particles are most likely monometallic Pd and are detrimental to the overall CO_2 selectivity.

High-temperature H_2 treatment of these catalysts has a dual role: to allow transformation of the Pd to PdZn and to eliminate the smallest Pd particles that are detrimental to overall CO_2 selectivity. As the PdZn alloy is formed, mean particle size increases. Surprisingly, we found that retaining smaller PdZn particles through lower-temperature reduction did not result in higher reactivity; catalysts with mean diameter of 9 nm were as reactive as those with mean diameter of 34 nm. This suggests that the support ZnO plays a significant role in the methanol steam-reforming reaction.

Acknowledgments

This work was supported by the U.S. Army Research Laboratory under the Collaborative Technology Alliance Program

(cooperative agreement DAAD19-01-2-0010) and by the U.S. Department of Energy (grant DE-FG02-05ER15712).

References

[1] J. Hu, Y. Wang, D. Van der Wiel, C. Chin, D. Palo, R. Rozmiarek, R. Dagle, J. Cao, J. Holladay, E. Baker, Chem. Eng. J. 93 (2003) 5560.
[2] L.F. Brown, Int. J. Hydrogen Energy 26 (2001) 381.
[3] O. Savadogo, B. Xing, J. New Mater. Electrochem. Syst. 3 (2000) 345.
[4] D. Trimm, Z. Onsan, Catal. Rev. 43 (2001) 31.
[5] N. Iwasa, S. Kudo, H. Takahashi, S. Masuda, N. Takezawa, Catal. Lett. 19 (1993) 211.
[6] N. Iwasa, S. Masuda, N. Ogawa, N. Takezawa, Appl. Catal. A Gen. 125 (1995) 145.
[7] N. Iwasa, N. Ogawa, S. Masuda, N. Takezawa, Bull. Chem. Soc. Jpn. 71 (1998) 1451.
[8] Y.-H. Chin, R. Dagle, J. Hu, A.C. Dohnalkova, Y. Wang, Catal. Today 77 (2002) 79.
[9] A. Karim, A comparison between packed bed and wall coated reactors for the steam reforming of methanol, Master's thesis, University of New Mexico, December 2003.
[10] N. Iwasa, N. Takezawa, Top. Catal. 22 (2003) 215.